COMPDYN 2011
3rd ECCOMAS Thematic Conference on
Computational Methods in Structural Dynamics and Earthquake Engineering
M. Papadrakakis, M. Fragiadakis, V. Plevris (eds.)
Corfu, Greece, 25–28 May 2011

DYNAMIC PERFORMANCE OF EXISTING HIGH-SPEED RAILWAY BRIDGES UNDER RESONANT CONDITIONS, RETROFITTED WITH FLUID-VISCOUS DAMPERS SUPPORTED ON CLAMPED AUXILIARY BEAMS

J. Lavado[1], M.D. Martinez-Rodrigo[2], and P. Museros[3]

[1] University of Granada, Dept. of Structural Mechanics and Hydraulic Engineering
18071 Granada, Spain
e-mail: jlavado@ugr.es

[2] University Jaume I, Dept. of Mechanical Engineering and Construction
12071 Castellon, Spain
e-mail: Lola.Martinez@emc.uji.es

[3] University Polytechnic of Valencia, Dept. of Cont. Medium Mechanics and Theory of Structures
46022 Valencia, Spain
e-mail: pmuseros@mes.upv.es

Keywords: Resonance in Railway Bridges, Passive Control of Structures, Double-beam System, Moving Loads, Dynamics of Bridges, Fluid-viscous Dampers.

Abstract. *In this contribution the application of Passive Control techniques is applied to reduce the severe transverse vibrations that railway bridges of moderate lengths may experiment under resonance conditions. The proposed solution consists on connecting the slab to a series of auxiliary beams with partially restrained rotational end conditions through a set of fluid-viscous dampers. A particular configuration minimizing the space occupied under the bridge deck by the devices and the auxiliary beams is proposed for slabs and girder bridges, typical typologies in the aforementioned range of lengths. First, the dynamic response of the double-beam system at resonance is obtained in closed-form under harmonic excitation in order to detect the main governing parameters of the bridge response. Then conditions for the optimal dampers constants and minimum beam sizes that minimize the bridge dynamic amplification at resonance are obtained using a planar analytical model. Finally the effectiveness of the solution and the adequacy of the expressions derived from the harmonic case are proven under railway traffic excitation. Special attention is given to the beneficial effect of partially restraining the auxiliary beam supports throughout the study.*

1 INTRODUCTION

The extensive construction of new High-Speed railway lines and the use of conventional lines for higher operating train velocities require the continuous upgrading of railway infrastructure and, in particular, of bridge structures. Even though modern trains' axle loads are not higher than old-time vehicles transmitted forces, higher design velocities may lead to the appearance of resonance phenomena. Resonance, in a railway bridge, takes place when the exciting frequency of the train's periodic loading becomes close to the natural frequency of the bridge. If this is the case, the loads enter the bridge in phase with the natural oscillations of the structure leading to a progressive increase of the deck transverse oscillations. If structural damping is low, as it usually is the case in railway bridges [1], and the number of axles is sufficient severe transverse vibrations at the platform area could build up causing the failure of the Serviceability Limit State of vertical acceleration [2]. Specially critical structures in this regard are short-to-medium-span bridges (12 to 25 m) where the main structural elements are simply-supported (S-S) beams or plates. In these structures resonance phenomena may cause not only impact or fatigue related damage but also failure of ballast-beds due to relaxation and scattering of ballasts. This can compromise the running safety of the trains, the ride comfort of passengers, and ultimately increase the bridge maintenance costs [1, 3, 4].

In existing bridges that experiment this kind of behavior, due to either an increase in the Maximum Line Speed at the site or to structural degradation with time, classical solutions could be applied such as increasing the mass of the deck and therefore reducing its acceleration or augmenting its stiffness and consequently raising its natural frequencies and critical velocities. Nevertheless in many circumstances it is not possible to preserve the original structure and the deck needs to be demolished and replaced with the subsequent interruption of the line services. Alternatively, in this contribution the reduction of the bridge dynamic response by artificially increasing the overall damping of the structure applying Passive Control techniques and, in particular, retrofitting the bridge deck with Fluid Viscous Dampers (FVDs) is proposed and evaluated.

Despite the fact that vibration control systems have been applied to reduce the dynamic response of structures since the 1960s, only a few authors have addressed the practical application of these technologies to bridges under the action of moving vehicles. The application of Tuned Mass Dampers (TMDs) to the train-induced vibration problem has been addressed by Kwon et al. [5], Wang et al. [6], Yau et al. [7, 8, 9] and Li et al. [10]. These authors investigate the dynamic performance of bridges using planar models retrofitted with single or multiple TMDs. TMDs are tuned to a single frequency of the superstructure (usually the fundamental one) or several frequencies which contributions need to be reduced. From these works it can be inferred that the vehicle passage time on the bridge is, in many circumstances, too short to build up the needed TMD vibrating regime that effectively mitigates the bridge excessive vibrations; besides, detuning problems may arise if the devices are tuned to the bridge natural frequency, due to the variability of this magnitude over time associated to vehicle-bridge interaction effects, changing environmental parameters (e.g. temperature), or to the decay of the TMD stiffness with time. Nevertheless this second drawback may be partially overcome with multiple TMDs tuned in a frequency interval [8, 10] or with the string-type TMD presented in [9]. Recently Samani [11] has compared the vibration reduction capability of nonlinear TMDs when compared to linear elements connected to simply-supported beams under moving loads concluding that the vibration reduction achieved levels are very similar.

Minsili et al. [12] suggest the installation of supplemental diagonal elements in truss bridges connected to the original braces through Slotted Friction Connections, in order to mitigate traffic and earthquake induced vibrations. The authors point out that with this alterna-

tive structural displacements can be reduced to a great extent, but vertical accelerations may exceed their initial values due to the nature of the new forces introduced in the bridge deck. The appearance of residual displacements in the structure after the devices activation is an additional inconvenient of the proposed system.

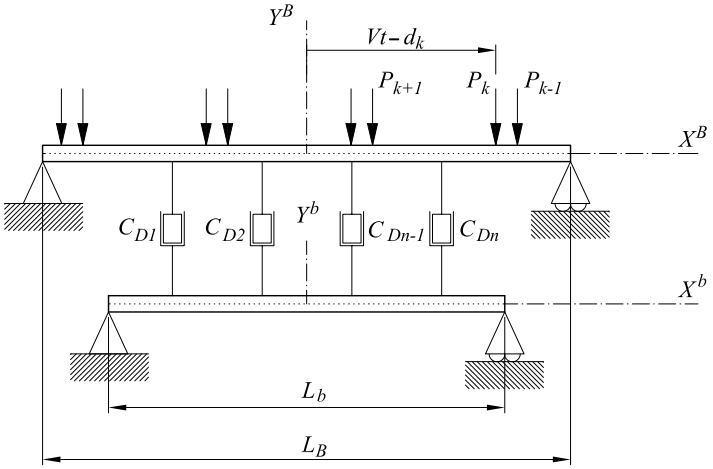

Figure 1: Simply-supported double beam system connected through FVDs and (b) simply-supported-partially-clamped double beam system connected through FVDs.

The use of viscoelastic (VE) materials to improve the dynamic performance of railway bridges has been addressed by a number of researchers. Choo et al. [13] propose the introduction of acrylic rubber patches connected to S-S beams deforming in shear when the main elements bend. The authors carry out an experimental program and adjust a numerical constitutive model for this material. They finally conclude that the proposed design could reduce to permitted levels the structural response of long span bridges which experience inadmissible vertical accelerations. A few authors have investigated the applicability of Continuous Dynamic Vibration Absorbers (CDVAs) combined with viscoelastic materials, to the vibration control of beams under harmonic and moving loads. Vu et al. [14] and Abu-Hilal [15] study the possibility of reducing the dynamic response of a Bernoulli-Euler (B-E) beam by connecting it to an identical element through a continuous layer of VE material. Onsizczuk analyses the dynamic behaviour of double-beam [16, 17] and double plate systems [18, 19] linked through continuous Winkler media focusing on the relative properties of the three elements that control the oscillations of the main element. Recently, Moliner et al. [20, 21] have investigated the dynamic performance of the double-beam system connected by discrete Kelvin elements and have evaluated its applicability in reducing the resonant response of short S-S railway bridges. A few authors have addressed the use of pure viscous dampers to reduce the amplification in beams traversed by moving vehicles. Oliveto et al. [22] and Greco et al. [23] solve the dynamic problem of a continuous beam with two end rotational viscous dampers under the circulation of a single load, by using an extension of the complex mode superposition method. Nevertheless, to the authors' knowledge, this type of damper has never been previously applied in the context of High-Speed railway traffic.

FVDs have been selected, as compared to other Passive Control devices for this application, because they dissipate energy at a wide scope of frequency ranges, and not only at narrow ranges like TMDs. As a consequence, they do not present relevant tuning and detuning drawbacks. A further advantage is the fact that dissipative devices based on friction or yielding increase replacement operations and maintenance costs. In contrast, some FVDs are equipped with labyrinth seals which eliminate mechanical friction [24], allowing them to undergo an enormous number of cycles before they have to be replaced. Moreover, since in FVDs the

maximum force and maximum displacement are out of phase, additional forces introduced in the structure are small when compared to other techniques.

The authors of this contribution have investigated in the past the dynamic behaviour of a double-beam system as the one shown in Fig. 1 linked through a distribution of pure FVDs under the circulation of moving loads [25, 26].

It consists of a *main beam*, which represents the bridge, and an *auxiliary beam* with simply-supported end conditions connected to the bridge by means of FVDs. Closed-form expressions for the optimal dampers minimising the bridge response have been provided, and a methodology for the auxiliary beam design has been developed based on the overall damping needs. This study has been completed accounting for the contribution of three-dimensional modes of the bridge, which cannot be neglected in multi-track decks or when the deck has a skew geometry. To this end the dynamic performance of orthotropic plates connected to auxiliary beams distributed along the deck width with, again, simply-supported end conditions through FVDs has been analysed in detail [25, 27, 28].

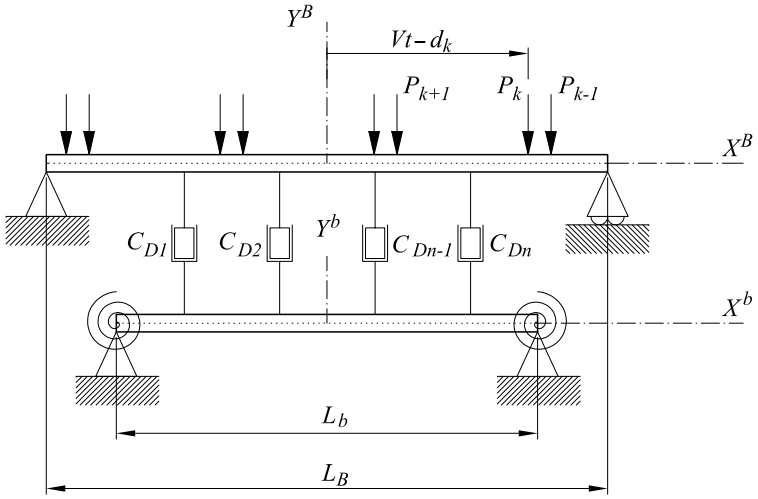

Figure 2: Simply-supported-partially-clamped double beam system connected through FVDs.

One of the main conclusions derived from the previous works by the authors is that in order for the FVDs to effectively reduce the deck vibratory response, the fundamental frequency of the auxiliary beam (lower beam in Fig. 1) needs to exceed the bridge or main beam highest frequency which contribution is to be controlled. Moreover, as the auxiliary beam frequency increases, the dissipative capacity of the system raises. Due to this condition the secondary beam needs always to be oversized when compared to the minimum beam that would accomplish resistance requirements under the dampers forces. As the proposed configuration, that is presented in section 2, consists on installing the retrofitting system below the slab the needed auxiliary beams may occupy an excessive portion of the free space under the deck. Furthermore, as current design standards [2, 29] prescribe to account for frequency contents up to 30 Hz in the computation of the deck transverse acceleration, modes close to 30 Hz are almost impossible to control with the proposed system because beams with fundamental frequencies exceeding 30 Hz require enormous section heights for spans in the neighborhood of 20-25 m. To overcome this problem a variation on the configuration of the retrofitting system already studied by the authors is proposed which consists on transforming the original simply-supported boundary conditions of the auxiliary beam restraining the extreme sections rotation. In an ideal case if the beam could be perfectly clamped at the ends the natural frequency of the fundamental mode would increase approximately 2.27 times with respect to simply-supported end conditions. As perfect clamping is not possible the system shown in Fig. 2 is

analyzed. This way the efficiency of the solution can be investigated in terms of the partial rotational restriction of the beam supports.

The objectives of the present study are (i) to propose a methodology to select the minimum size of the auxiliary beam and optimum FVDs constants minimizing the dynamic response of the main simply-supported beam at resonance; (ii) to prove that with the proposed solution severe levels of vertical acceleration may be drastically reduced without exceeding the devices maximum bearing capacity, the maximum admissible stress in the beams nor the punching force in the slab, and (iii) to evaluate the beneficial effect of partially clamping the auxiliary beam supports when compared to the previously analyzed simply-supported case.

2 CONFIGURATION OF THE DAMPING SYSTEM

The dissipative system to be installed on the beam supporting the passage of the loads consists of two main elements. The first element is an auxiliary, partially clamped beam which in typical applications is generally located underneath the main one.

The second element is a set of FVDs linking the vertical motion of certain sections of the main beam and the auxiliary one. Our attention here is focused on mitigating the flexural vibrations of the main beam when the train of moving loads induces a resonance situation. For this reason, the planar model shown in Fig. 2 is used to analyse the performance of the proposed retrofit alternative. For the sake of simplicity two Cartesian coordinate systems are introduced with origins located at both beams mid-span sections.

The loads acting on the structure are assumed to be constant-valued, i.e. vehicle–bridge interaction effects are neglected. Also, the main beam is assumed to rest directly on the abutments without any intermediate elastic bearing.

The torsional oscillations experienced by beams subjected to eccentric moving loads are not accounted for in the analytical formulation and optimisation of this study. Consequently, the results presented in sections 2 and 3 are not applicable to either multi-track or single-track skewed railway bridges. However, it should be emphasised that single-track non-skewed bridges, and in particular, medium to short-span ones are some of the most unfavourable cases found in practice. As a consequence of their low total mass, this type of structures may undergo severe resonant oscillations under the passage of fast trains, thus generating highly demanding situations for any dissipative system.

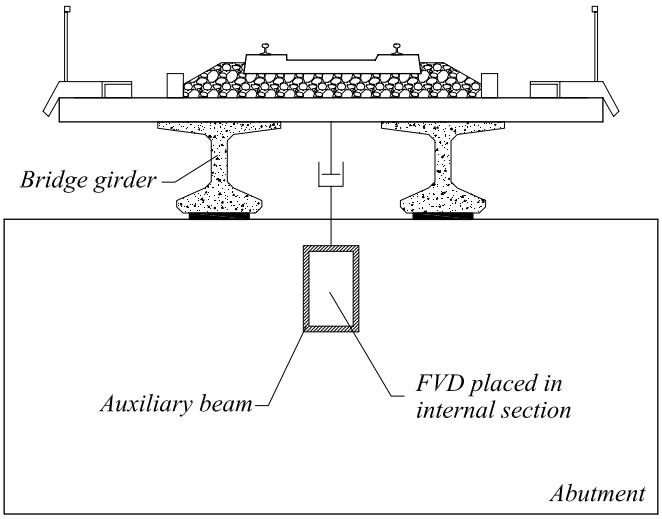

Figure 3: Retrofit configuration for a concrete girders bridge deck.

Fig. 3 shows a possible configuration of the auxiliary beam and dampers installed in a sin-

gle-track railway bridge. The dampers link the lower side of the slab and the upper flange of an auxiliary beam with hollow rectangular cross-section. The auxiliary beam is clamped on the abutments at the outermost sections of the bridge. Other suitable configurations could be adopted for different auxiliary beams geometries and deck typologies with an essential dynamic behaviour as that represented in Fig. 2.

3 GOVERNING PARAMETERS AND INFLUENCE ON THE RESPONSE

3.1 Equations of motion of a simple beam under moving loads

The partial differential equation governing the flexural behaviour of a simply supported beam (main beam of the system) subjected to a train of concentrated loads can be found in the works of several authors such as Frýba [30, 31], Olsson [32], Yang et al. [33] and Museros and Alarcón [34]. Neglecting the effects of shear deformation and rotary inertia, and considering that the loads are aligned with the axis of symmetry of the cross-section (Y axis), the governing equation can be written as

$$m\frac{\partial^2 y}{\partial y^2}+\frac{\partial^2}{\partial x^2}\left(EI\frac{\partial^2 y}{\partial x^2}\right)=q(x,t). \tag{1}$$

In Eq. (1) the following notation is used: m is the mass per unit length, $y = y(x,t)$ the transverse displacement of any beam section at time t, x refers to the longitudinal coordinate, E is the Modulus of Elasticity, I the second moment of area of the cross-section and $q(x,t)$ stands for the distributed load per unit length acting at time t (positive if directed upwards).

The deformed shape is expressed as a linear combination of a family of sines and cosines $\phi_j(x)$ as in Eq. (2), where N_{mod} stands for the number of modes considered, $\xi_j(t)$ is the amplitude of the jth mode, and L is the length of the beam.

$$y(x,t)=\sum_{j=1}^{N_{\mathrm{mod}}}\xi_j(t)\cdot\phi_j(x) \quad \text{where} \quad \phi_j(x)=\begin{cases}\cos\left(\dfrac{j\pi x}{L}\right) & \text{if} \quad j=\text{odd number}\\ \sin\left(\dfrac{j\pi x}{L}\right) & \text{if} \quad j=\text{even number}\end{cases} \tag{2}$$

The loads are represented by means of Dirac delta functions acting at $x = Vt–d_k$, where V is the constant train speed, and d_k is the original distance from the kth load to the mid-span section of the beam. Thus, $q(x,t)$ may be expressed as follows:

$$q(x,t)=-\sum_{k=1}^{N_P}\left(H\left(t-\frac{d_k}{V}\right)-H\left(t-\frac{d_k+L}{V}\right)\right)P_k\delta\left(x-\left(Vt-d_k\right)\right), \tag{3}$$

where N_P is the total number of axle loads; P_k is the value of the kth load; and $H(t–t_0)$ is the Heaviside unit function acting at time t_0. When Eqs. (2) and (3) are introduced in Eq. (1), and multiplication by the nth function $\phi_n(x)$ and integration along the span L are carried out, the nth modal equation of motion is obtained. To this end, the mass per unit length m and the flexural stiffness EI are assumed to be constant along the beam. Introducing a modal viscous damping ratio ζ_n, the modal equation of motion is expressed as

$$\ddot{\xi}_n(t)+2\zeta_n\omega_n\dot{\xi}_n(t)+\omega_n^2\xi_n(t)=\frac{-2}{mL}\sum_{k=1}^{N_P}\left(H\left(t-\frac{d_k}{V}\right)-H\left(t-\frac{d_k+L}{V}\right)\right)P_k\cos\frac{n\pi\left(Vt-d_{k)}\right)}{L}, \tag{4}$$

where over-dots indicate differentiation with respect to time, and ω_n represents the nth circular frequency of the main beam in rad/s

$$\omega_n = \left(\frac{n\pi}{L}\right)^2 \sqrt{\frac{EI}{m}}. \tag{5}$$

3.2 Governing equations of the beam equipped with fluid viscous dampers and subjected to moving loads

In this section the equations of motion of the double-beam system are formulated as the auxiliary beam is connected to the main one through the dampers distribution.

The auxiliary beam is partially clamped, therefore, the boundary conditions of the secondary beam are considered to be simply supported with two identical rotational springs at both ends. The partial differential equation governing the flexural behaviour of the auxiliary beam has the same general expression than that of a simply supported element Eq. (1).

When the auxiliary beam is connected to the main one by means of the FVDs, the equations of motion must be suitably modified. In practical applications, resonance induced by constant moving loads is a problem of bridges subjected to the passage of fast trains. Museros and Alarcón [34] show that resonance of the second bending mode can take place in certain cases but, in single-track bridges it is most likely that resonance will be related to oscillations of the first bending mode. This is a consequence of the maximum speed attainable by modern high-speed trains. Under such circumstances, the influence of modes other than the one undergoing resonance can be disregarded for the computation of the main beam response.

The oscillations of the first mode of the main beam at resonance tend to create a symmetric distribution of dampers forces with respect to the mid-span section. These forces excite the movement of the auxiliary beam which, consequently, can be initially analysed only taking into account the contribution of its first bending mode as well. The viability of disregarding the second and higher modes of the beams in the calculation of the optimal parameters of the damping system is subsequently verified in section 5.

If the deformed shape of the auxiliary beam is expressed as the product of a modal amplitude times its first modal shape:

$$y(x,t) = \xi_1(t)\cdot\phi_1(x) = \xi_1(t)\cdot\left(\frac{\cosh\left(\frac{\beta\cdot L}{2}\right)\cdot\cos(\beta\cdot x)}{\cosh\left(\frac{\beta\cdot L}{2}\right)-\cos\left(\frac{\beta\cdot L}{2}\right)} - \frac{\cos\left(\frac{\beta\cdot L}{2}\right)\cdot\cosh(\beta\cdot x)}{\cosh\left(\frac{\beta\cdot L}{2}\right)-\cos\left(\frac{\beta\cdot L}{2}\right)}\right) \tag{6}$$

where β is:

$$\beta = \sqrt[4]{\frac{\omega_1^{\,2}\cdot m}{E\cdot I}}. \tag{7}$$

In expression (7) ω_1 represents the first circular frequency of a simply-supported beam with rotational springs, in rad/s, which can be computed from the lowest root of the frequency equation:

$$\begin{aligned} -\frac{(\beta L)^2}{4}\sinh(\beta L)\sin(\beta L) + \bar{K}\beta L\sinh(\beta L)\cos(\beta L) - \\ -\bar{K}\beta L\cosh(\beta L)\sin(\beta L) + 2\bar{K}^2\cosh(\beta L)\cos(\beta L) - 2\bar{K}^2 = 0 \end{aligned} \tag{8}$$

being $\bar{K}$ a stiffness ratio between the rotational springs constants and the beam bending stiffness defined as

$$\bar{K} = \frac{KL}{4EI}. \tag{9}$$

Considering therefore only the contribution of the fundamental modes of both beams, the resulting equations of motion of the double-beam system linked by the distribution of the dampers in modal space are as follows:

$$\tilde{m}_B\ddot{\xi}_B(t)+2\zeta_B\omega_B\tilde{m}_B\dot{\xi}_B(t)+C_D^{BB}\dot{\xi}_B(t)-C_D^{Bb}\dot{\xi}_b(t)+\tilde{K}_B\xi_B(t)=q(x,t) \tag{10a}$$

$$\tilde{m}_b\ddot{\xi}_b(t)+2\zeta_b\omega_b\tilde{m}_b\dot{\xi}_b(t)+C_D^{bb}\dot{\xi}_b(t)-C_D^{Bb}\dot{\xi}_B(t)+\tilde{K}_b\xi_b(t)=0 \tag{10b}$$

$$q(x,t)=-\sum_{k=1}^{N_p}\left(H\left(t-\frac{d_k}{V}\right)-H\left(t-\frac{d_k+L_B}{V}\right)\right)P_k\cos\frac{n\pi(Vt-d_k)}{L_B} \tag{10c}$$

The notation in Eq. (10) is analogous to previous equations but with superscripts and subscripts *B* and *b*, which are included to indicate magnitudes associated to the main and auxiliary beam, respectively. Moreover, in equation (10):

$$\tilde{m}_B=\frac{m_BL_B}{2} \quad \text{is the first modal mass for the main beam} \tag{11}$$

$$\tilde{K}_B=\frac{\omega_B^2m_BL_B}{2} \quad \text{is the first modal stiffness for the main beam} \tag{12}$$

$$\tilde{m}_b=m_b\cdot c \quad \text{is the first modal mass for the auxiliary beam, where:} \tag{13}$$

$$c=\frac{L_b\cdot\left[2\gamma+\gamma\cos\gamma+\cosh\gamma(\gamma-\sin\gamma)-\sin\gamma-(1+\cos\gamma)\sinh\gamma\right]}{4\gamma\left[\cos\left(\frac{\gamma}{2}\right)-\cosh\left(\frac{\gamma}{2}\right)\right]^2} \tag{14}$$

$$\gamma=\beta L_b \tag{15}$$

$$\tilde{K}_b=\left(\frac{\gamma}{L_b}\right)^4\cdot c\cdot E_b\cdot I_b \tag{16}$$

$$C_D^{BB}=\sum_{i=1}^{N_D}C_{Di}\cdot\left(\cos\left(\frac{\pi x_{Di}^B}{L_B}\right)\right)^2 \tag{17}$$

$$C_D^{Bb}=\sum_{i=1}^{N_D}C_{Di}\cdot\cos\left(\frac{\pi x_{Di}^B}{L_B}\right)\cdot\left[A\cdot\cosh\left(\frac{\gamma\cdot x_{Di}^b}{L_b}\right)+B\cdot\cos\left(\frac{\gamma\cdot x_{Di}^b}{L_b}\right)\right] \tag{18}$$

$$C_D^{bb}=\sum_{i=1}^{N_D}C_{Di}\cdot\left[A\cdot\cosh\left(\frac{\gamma\cdot x_{Di}^b}{L_b}\right)+B\cdot\cos\left(\frac{\gamma\cdot x_{Di}^b}{L_b}\right)\right]^2 \tag{19}$$

Notice that parameter γ is a function of the quotient between the auxiliary partially clamped beam circular frequency and the same beam frequency with simply-supported end conditions:

$$\gamma=\beta L_b=\pi\sqrt{\frac{\omega_b}{\omega_{b,ss}}} \tag{20}$$

In expressions (17), (18) and (19), C_{Di} is the constant of the *i*th damper. The location of the *i*th damper is designated as x^B_{Di} along the X^B axis of the main beam, and as x^b_{Di} along the X^b axis of the auxiliary beam. The significance of parameters A and B is:

$$A = \frac{-\cos\left(\frac{\gamma}{2}\right)}{\cosh\left(\frac{\gamma}{2}\right)-\cos\left(\frac{\gamma}{2}\right)} \qquad B = \frac{\cosh\left(\frac{\gamma}{2}\right)}{\cosh\left(\frac{\gamma}{2}\right)-\cos\left(\frac{\gamma}{2}\right)} \tag{21}$$

From Eqs. (10) it can be seen that, if the modal system of equations is written in matrix form, the load term associated to the forces exerted by the FVDs gives rise, in general, to a full damping matrix.

3.3 Nondimensional formulation of the system under harmonic excitation

This article focuses on the reduction of the resonant response of beams or bridges, and therefore the system shown in Fig. 2 will first be analysed under the action of a harmonically varying force applied at the mid-span section of the main beam (see Fig. 4a). This kind of excitation captures the essential features of the system response at resonance.

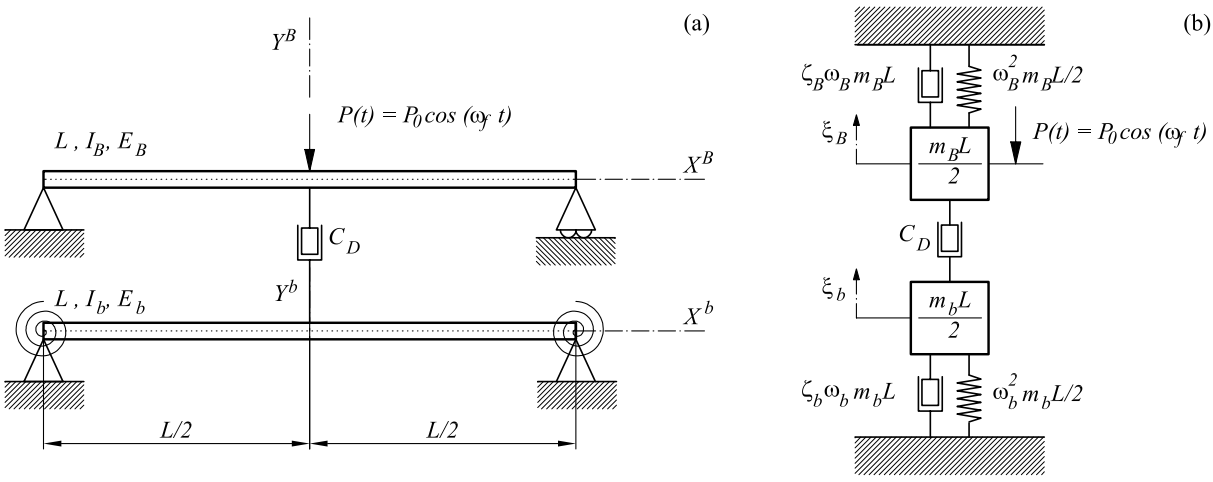

Figure 4: (a) Double-beam system under harmonic excitation applied at mid-span. (b) Equivalent 2dof system in modal space.

In what follows, it will be assumed that the lengths of both beams are equal, $L_B = L_b = L$ and the main and auxiliary beams are vertically aligned so that $x^B_{Di} = x^b_{Di}$, i = 1, 2, ... N_D. These hypotheses are the most relevant ones for real applications because it is most likely that in actual bridges, the auxiliary beam or beams are supported at the original abutments or close to them. If only the first mode of both beams is taken into account, any number of FVDs located at different sections is equivalent to a single equivalent FVD located at mid-span with equivalent damping constant:

$$C_D = \sum_{i=1}^{N_D} C_{Di} \cdot \left(\cos\left(\frac{\pi x^B_{Di}}{L_B}\right)\right)^2 \tag{22}$$

Under the aforementioned circumstances, the response in terms of modal amplitudes corresponds to that of the two-degree-of-freedom (2dof) system shown in Fig. 4b, where ξ_B and ξ_b, are the first modal amplitudes of the main and auxiliary beam, respectively.

The equations of motion of the system may be expressed as:

$$\begin{bmatrix} \tilde{m}_B & 0 \\ 0 & \tilde{m}_b \end{bmatrix} \cdot \begin{pmatrix} \ddot{\xi}_B \\ \ddot{\xi}_b \end{pmatrix} + \begin{bmatrix} 2\zeta_B \omega_B \tilde{m}_B + C_D^{BB} & -C_D^{Bb} \\ -C_D^{Bb} & 2\zeta_b \omega_b \tilde{m}_b + C_D^{bb} \end{bmatrix} \cdot \begin{pmatrix} \dot{\xi}_B \\ \dot{\xi}_b \end{pmatrix} + \begin{bmatrix} \tilde{K}_B & 0 \\ 0 & \tilde{K}_b \end{bmatrix} \cdot \begin{pmatrix} \xi_B \\ \xi_b \end{pmatrix} = \begin{pmatrix} -P_0 \cos\left(\omega_f t\right) \\ 0 \end{pmatrix} \tag{23}$$

In Eq. (23) P_0 and ω_f are the amplitude and the forcing frequency of the excitation, respectively. In order to solve Eq. (23) the following dimensionless ratios are defined:

$$\text{Frequency ratio:} \quad \eta = \omega_b / \omega_B \tag{24a}$$

$$\text{Excitation frequency ratio:} \quad \Omega = \omega_f / \omega_B \tag{24b}$$

$$\text{Mass ratio:} \quad \mu = m_b / m_B \tag{24c}$$

$$\text{Supplemental damping ratio:} \quad \zeta_D = C_D / (m_B L \omega_B) \tag{24d}$$

Moreover, when there is only a single equivalent FVD located at mid-span, with $x_D{}^B = x_D{}^b = 0$ parameters $C_D{}^{BB}$, $C_D{}^{Bb}$ and $C_D{}^{bb}$ become equal:

$$C_D^{BB} = \sum_{i=1}^{N_D} C_{Di} \cdot \left(\cos\left(\frac{\pi x_{Di}^B}{L_B} \right) \right)^2 = C_D \tag{25}$$

$$C_D^{Bb} = \sum_{i=1}^{N_D} C_{Di} \cdot \cos\left(\frac{\pi x_{Di}^B}{L_B} \right) \cdot \left[A \cdot \cosh\left(\frac{\gamma \cdot x_{Di}^b}{L_b} \right) + B \cdot \cos\left(\frac{\gamma \cdot x_{Di}^b}{L_b} \right) \right] = C_D \cdot [A + B] = C_D \tag{26}$$

$$C_D^{bb} = \sum_{i=1}^{N_D} C_{Di} \cdot \left[A \cdot \cosh\left(\frac{\gamma \cdot x_{Di}^b}{L_b} \right) + B \cdot \cos\left(\frac{\gamma \cdot x_{Di}^b}{L_b} \right) \right]^2 = C_D \cdot [A + B]^2 = C_D \tag{27}$$

Rewriting Eq. (23) in terms of the dimensionless ratios defined in Eqs. (24) yields

$$\begin{bmatrix} 1 & 0 \\ 0 & \mu \end{bmatrix} \cdot \begin{pmatrix} \ddot{\xi}_B \\ \ddot{\xi}_b \end{pmatrix} + 2\omega_B \begin{bmatrix} \zeta_B + \zeta_D & -\zeta_D \\ -\zeta_D & \zeta_b \eta \mu + \zeta_D \end{bmatrix} \cdot \begin{pmatrix} \dot{\xi}_B \\ \dot{\xi}_b \end{pmatrix} + \omega_B^2 \begin{bmatrix} 1 & 0 \\ 0 & \eta^2 \mu \end{bmatrix} \cdot \begin{pmatrix} \xi_B \\ \xi_b \end{pmatrix} = \begin{pmatrix} \dfrac{-2P_0}{m_B L} \cos(\omega_f t) \\ 0 \end{pmatrix} \tag{28}$$

Equation (28) written in terms of the nondimensional parameters is equivalent to that of the double-beam system with simply-supported end conditions in both beams previously analysed by the authors in reference [26]. Assuming again that the maximum response of the main beam will take place at resonance the transient solution is neglected and the dynamic amplification of the response is obtained for both beams as:

$$\begin{pmatrix} \overline{\xi}_B \\ \overline{\xi}_b \end{pmatrix} = \left(-\omega_f^2 \mathbf{M} + i\omega_f \mathbf{C} + \mathbf{K} \right)^{-1} \cdot \begin{pmatrix} \dfrac{-2P_0}{m_B L} \\ 0 \end{pmatrix} \tag{29}$$

where $\overline{\xi}_B$ and $\overline{\xi}_b$ are the complex amplitudes, **M**, **C** and **K** are the mass, damping and stiffness modal matrices from Eq. (28), and $i = \sqrt{-1}$. The moduli of $\overline{\xi}_B$ and $\overline{\xi}_b$ give the amplitudes of the response. In order to obtain a dimensionless representation of the beams response, two modal amplifications are defined as the modulus of $\overline{\xi}_B$ and $\overline{\xi}_b$ divided by the static deflection caused by the concentrated load P_0 acting on the main beam

$$A_B = \frac{\left| \overline{\xi}_B \right|}{2P_0 / \left(\omega_B^2 m_B L \right)} \tag{30a}$$

$$A_b = \frac{\left| \overline{\xi}_b \right|}{2P_0 / \left(\omega_B^2 m_B L \right)} \tag{30b}$$

After some algebraic manipulation, the modal amplifications are obtained

$$A_B = \sqrt{\frac{4\Omega^2\left(\zeta_b\eta\mu+\zeta_D\right)^2+\mu^2\left(\eta^2-\Omega^2\right)}{E^2+4\Omega^2F^2}} \tag{31a}$$

$$A_b = \frac{2\Omega\zeta_D}{\sqrt{E^2+4\Omega^2F^2}} \tag{31b}$$

being

$$E = \mu\left(1-\Omega^2\right)\left(\eta^2-\Omega^2\right)+4\Omega^2\left(\zeta_D^2-\left(\zeta_B+\zeta_D\right)\left(\zeta_b\eta\mu+\zeta_D\right)\right) \tag{31c}$$

$$F = \left(1-\Omega^2\right)\left(\zeta_b\eta\mu+\zeta_D\right)+\mu\left(\zeta_B+\zeta_D\right)\left(\eta^2-\Omega^2\right) \tag{31d}$$

The main beam modal acceleration is also of great interest because of its relation with ballast stability, as mentioned in section 1. In the steady-state the amplitude of the acceleration a_B is

$$a_b = \left|\bar{\xi}_B\right|\omega_f^2 = \frac{2P}{m_BL}\Omega^2A_B \tag{32}$$

Eq. (31) shows that the amplification of the main beam response A_B, depends on the following six parameters: Ω, η, μ, ζ_D, ζ_b, ζ_B. Additionally, from Eq. (32) it can be seen that the modal acceleration of the main beam is inversely proportional to its total mass m_BL. The behaviour of the system in terms of these parameters is analysed in detail in the following section.

4 RETROFITTING SYSTEM OPTIMISATION

4.1 Optimal value of the supplemental damping ratio

The key variables of the problem that should be minimised are the main beam dynamic amplification and modal acceleration, A_B and a_B. In order to visualise how the governing parameters affect these magnitudes and determine what is the best selection of the auxiliary beam and damper for a particular bridge, a number of plots are included in Fig. 5.

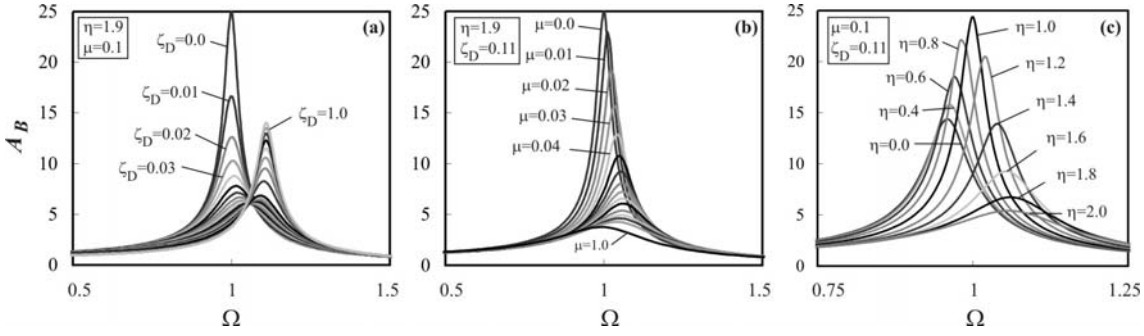

Figure 5: Main beam amplification A_B versus Ω for different values of ζ_D, μ and η.

The plots illustrate the evolution of the main beam resonant amplification with μ, η, and ζ_D. In all the cases structural dampings of the main and secondary beams are 2% and 0.5%, respectively. In Fig. 5a μ and η are fixed and equal to 0.1 and 1.9, respectively. In this plot, for a particular bridge and auxiliary beam the resonant response of the former is analyzed as the damper constant increases. As it can be seen, there is an optimum value of the damper constant which, for a particular auxiliary beam, leads to the minimum response of the main element. In Fig. 5b it is shown how the main beam amplification at resonance monotonically

diminishes with the auxiliary beam mass for fixed values of this element natural frequency and damper constant. Finally, in Fig. 5c the evolution of A_B with the frequency ratio η of the two beams fundamental frequency is evaluated. From the analysis of this plot it can be concluded that in order for the retrofitting system to effectively reduce the dynamic response of the main beam, η has to be higher than one, that is, the secondary beam natural frequency must exceed the main beam frequency. The system hardly dissipates energy when η=1. For values of η<1 the secondary beam and damper behave in a certain way as a Tuned Mass Damper and the main beam resonant response partially reduces but this reduction can reach much higher levels for values of η>1. When η tends to infinity, A_B monotonically decreases as in this case the damper lower end tends to be attached to a fixed reference (the same occurs when $\mu \to \infty$). From this situation the clear advantage of partially clamping the auxiliary beam ends is evident as it leads to an increase of the secondary beam frequency and a reduction of the main beam resonant response.

In conclusion, as there are not optimal values of η and μ, or in other words, the dissipation capacity of the system increases with increasing values of any of these two parameters, the design strategy should be to select the smallest auxiliary beam such that with its associated optimal damper provides enough energy dissipation to achieve the desired target performance. In what follows, a closed form expression for the optimal supplemental damping ratio ζ_D is obtained.

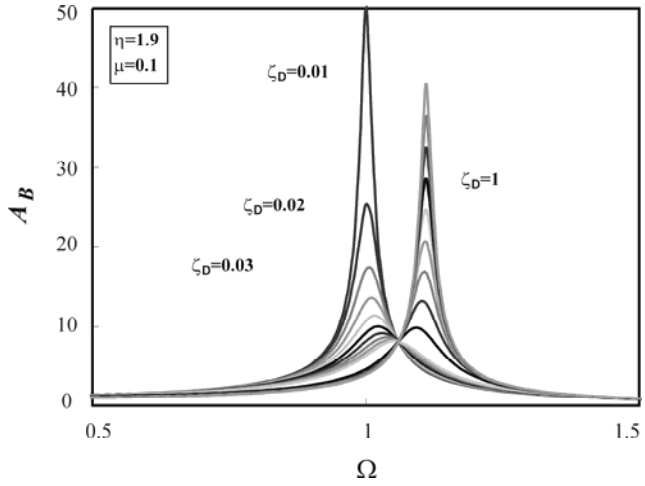

Figure 6: Main beam amplification A_B versus Ω for different values of ζ_D neglecting structural damping.

From the works of the European Rail Research Institute [1] it can be concluded that damping ratios in modern railway bridges are usually small, of the order of 1% or 2%, or even smaller in composite or metallic bridges. Therefore, in most practical cases an approximate solution to the problem can be obtained by assuming that structural damping is negligible in comparison with the dissipation introduced by the external FVD. This hypothesis allows the computation of a closed form expression for the optimal value of ζ_D. The subsequent numerical examples will prove the soundness of this approach. Neglecting structural damping, that is $\zeta_B = \zeta_b = 0$, Eqs. (31a), (31c) and (31d) transform into

$$A_B = \sqrt{\frac{4\Omega^2\zeta_D^2 + \mu^2\left(\eta^2-\Omega^2\right)^2}{\left(1-\Omega^2\right)^2\mu^2\left(\eta^2-\Omega^2\right)^2 + 4\Omega^2\zeta_D^2\left[1-\Omega^2+\mu\left(\eta^2-\Omega^2\right)\right]^2}} \tag{33}$$

Comparing Figs. 5a and 6 the effect of structural damping on the response can be observed.

The maximum amplification for low and high values of ζ_D at resonance reaches a much higher level when structural damping is neglected as in Fig. 6, but two important facts must be highlighted. First, the difference between the maximum amplifications is much lower when ζ_D takes the optimal value. This fact reveals that, if structural damping is low and the optimal value of ζ_D is selected, the greater part of the energy at resonance is dissipated through the FVD. Secondly, if structural damping is neglected as in Fig. 6, A_B is independent of ζ_D at the value of Ω corresponding to the minimum maximum. This fact permits the computation of the excitation frequency ratio at the minimum maximum Ω_R^*:

$$\Omega_R^* = \frac{1}{2+\mu}\sqrt{(2+\mu)\left(2+\mu\eta^2\right)} \tag{34}$$

and the subsequent derivation of closed-form expressions for the optimal damping ratio ζ_D minimising the main beam amplification and acceleration responses:

$$\frac{\partial A_B}{\partial \Omega}\left(\Omega=\Omega_R^*, \zeta_D=\zeta_{D,A}^*\right)=0 \quad \rightarrow \quad \zeta_{D,A}^* = \frac{\left(\eta^2-1\right)\mu}{\sqrt{4+6\mu+2\mu^2+2\mu\eta^2+3\mu^2\eta^2+\mu^3\eta^2}} \tag{35a}$$

$$\frac{\partial a_B}{\partial \Omega}\left(\Omega=\Omega_R^*, \zeta_D=\zeta_{D,a}^*\right)=0 \quad \rightarrow \quad \zeta_{D,a}^* = \frac{\left(\eta^2-1\right)\mu}{\sqrt{4+2\mu+6\mu\eta^2+3\mu^2\eta^2+2\mu^2\eta^4+\mu^3\eta^4}} \tag{35b}$$

Substituting the damping ratios given by Eqs. (35) into Eq. (24d), the associated optimal damper constants are obtained when structural damping is neglected. These equations provide optimum *equivalent* dampers, which are related to a particular longitudinal distribution of FVDs as per (22). In reference [26] a comprehensive analysis proving the adequacy of expressions (35) when structural damping is not neglected has been performed under harmonic conditions. Finally, in the example of a bridge retrofitted with the system proposed herein that is included in section 5 it is proven that these expressions predict dampers constants real optima with a great degree of accuracy under railway traffic, accounting for modal contributions higher than the fundamental one and including the presence of structural damping.

4.2 Effect of partial rotational restriction at the auxiliary beam supports

In this section the effect of partially restraining the auxiliary beam ends is analysed in terms of the reduction of the main beam resonant response attained as that obtained with a simply-supported auxiliary element. In order to isolate the boundary conditions alteration effect from the secondary beam size, the frequency ratio η is expressed as:

$$\eta = \frac{\omega_{b,ss}}{\omega_B}\left(\frac{\gamma}{\pi}\right)^2 = \eta_{ss,B}\left(\frac{\gamma}{\pi}\right)^2 \tag{36}$$

where $\omega_{b,ss}$ is the auxiliary beam circular frequency with hypothetical simply-supported end conditions and γ varies from π in the simply-supported case to 4.73004074 in the clamped case. In Fig. 7a curves of A_B associated to optimal values of the damping ratio $\zeta_{D,A}^*$ versus Ω have been plotted for a particular pair of beams (μ=0.1, $\eta_{ss,B}$=1.2, ζ_B=2% and ζ_b=0.5%) for increasing levels of rotational restriction of the secondary beam.

In order to measure these levels, instead of using the frequency parameter γ, the increase experimented by the auxiliary beam fundamental frequency with respect to the simply-supported case is employed defining to this end the following ratio:

$$\eta_{b,ss} = \frac{\omega_b}{\omega_{b,ss}} = \left(\frac{\gamma}{\pi}\right)^2 \tag{37}$$

Values of $\eta_{b,ss}$ increase from unity when the beam is simply supported towards 2.267 in the ideal case of a perfectly clamped beam. In order to be conservative it is considered that with nowadays constructive technologies and materials the maximum increase in the secondary beam frequency that can be attained clamping it is 1.5 times. In Fig. 7a $A_B(\Omega)$ has been plotted in the unretrofitted case for comparison purposes. The remaining curves correspond to the minimum response of the main beam at resonance (for optimal damping values $\zeta^*_{D,A}$) for a particular pair of beams and increasing values of γ (and therefore $\eta_{b,ss}$). The amplification at resonance is reduced from 25 to 16.3 when the auxiliary beam is simply supported, which entails a 34.8% reduction with respect to the unretrofitted case. This reduction increases with the restriction of the beam end rotations achieving 73.4% for $\eta_{b,ss}$=1.5. In other words, the main beam response is reduced in more than twice when, due to the auxiliary beam rotational springs stiffenning, the fundamental frequency of this element increases 50%. As we move towards the ideal case of a doubly clamped beam, this reduction tends to 88.6%. The interesting side of this alternative when compared to the simply-supported case previously analysed by the authors, is that the auxiliary beam size if partially clamped can be drastically reduced for the same main beam dynamic performance. If the beams are to be installed under the bridge deck in a practical application this is a crucial issue in order to minimise the free space occupied with the retrofit. Fig. 7b is similar to Fig. 7a but in this case the natural frequency of the secondary beam without restraining the ends rotations is higher ($\eta_{ss,B}$ = 1.6).

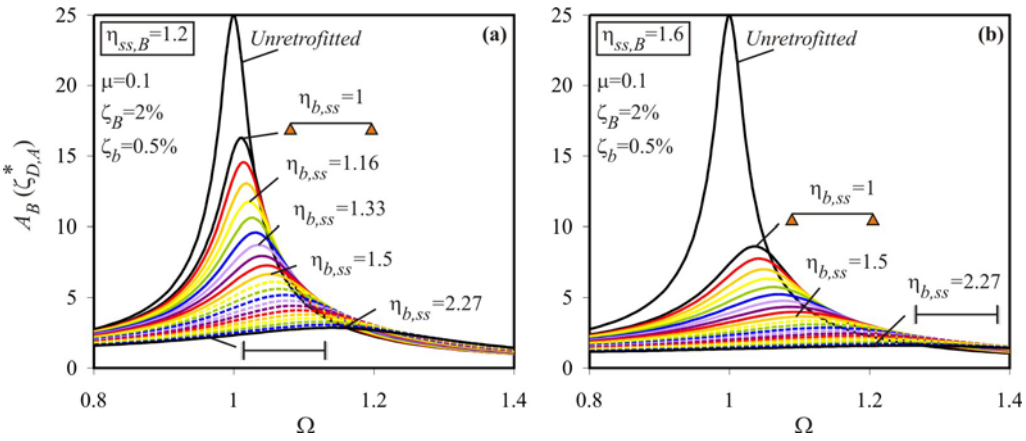

Figure 7: Main beam amplification A_B associated to the optimal damping ratio versus Ω for different clamping states of the auxiliary beam.

In order to visualize how the main beam response at resonance evolves with a particular auxiliary beam, always combined with the optimal equivalent damper, as the end rotational stiffness increases for different values of $\eta_{ss,B}$ the ratio R_{max} is defined measuring the reduction of the main beam maximum response achieved with the retrofit when compared to the unretrofitted case:

$$R_{max}(\%) = \frac{A^{\max}_{B,unret} - A^{\max}_{B}\left(\zeta_D = \zeta^*_{D,A}\right)}{A^{\max}_{B,unret}} \cdot 100 \tag{38}$$

where $A^{\max}_{B,unret}$ is the amplification of the main beam at resonance in the unretrofitted case and $A^{\max}_{B}\left(\zeta_D = \zeta^*_{D,A}\right)$ is the amplification of the main beam retrofitted with a particular auxiliary

beam in the optimal case. In other words, $A_B^{\max}\left(\zeta_D = \zeta_{D,A}^*\right)$ is the minimum response of the main beam at resonance that can be obtained with a particular auxiliary beam. This variable is calculated fixing the value of $\eta_{ss,B}$, i.e. for a particular auxiliary beam with a particular natural frequency and lineal mass and recalculated as the rotational restriction at the beam ends increases towards the fully clamped case. Therefore only the degree of clamping of the auxiliary beam is modified. In Fig. 8, plots (a), (b), (c) and (d) correspond to values of $\eta_{ss,B}$ {1, 1.2, 1.4, 1.6}and in each graph each curve has been calculated with a different level of the main beam structural damping.

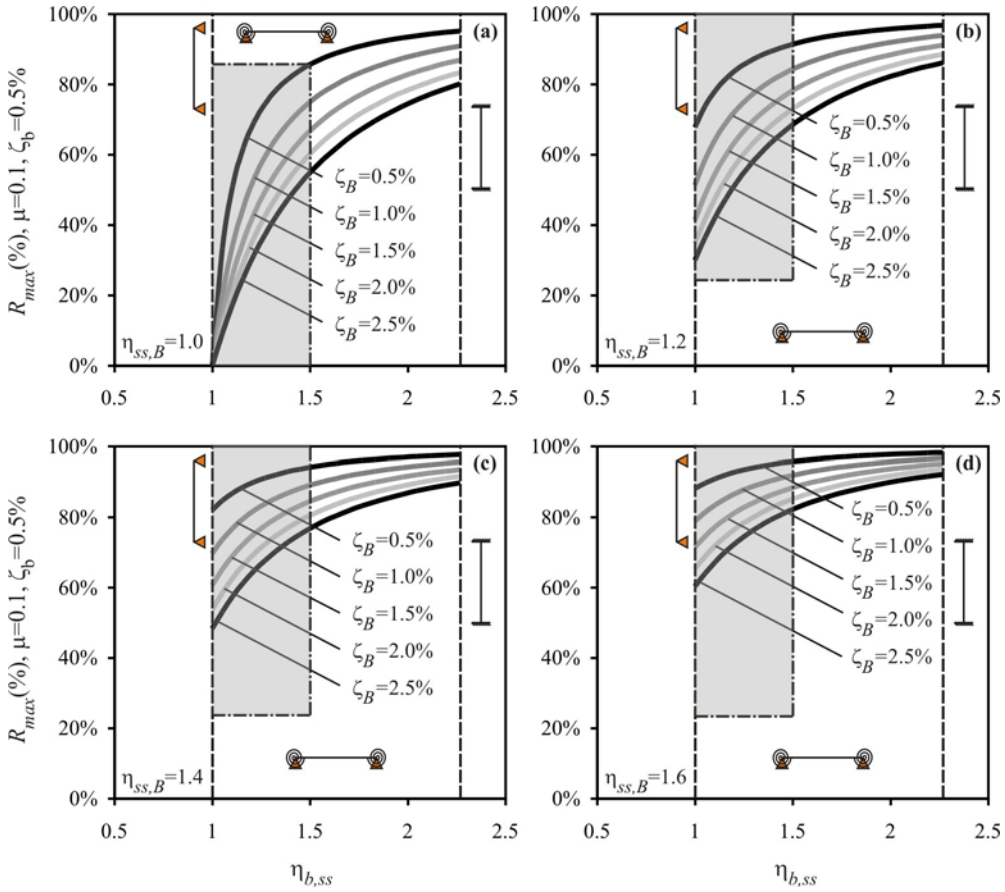

Figure 8: Maximum reduction with respect to the unretrofitted case vs. auxiliary beam frequency increase $\eta_{b,ss}$ due to supports rotational restriction.

In graph (a) $\eta_{ss,B}$=1, therefore prior to starting to clamp the secondary beam both beams have the same natural frequency. Due to this fact the retrofitting system efficiency is practically inexistent (see Fig. 5c) and the reduction of the main beam response is almost null. That is why for $\eta_{b,ss}$=1 (auxiliary beam simply-supported) all the curves tend to R_{max}=0. As the rotational restriction at the ends increases and therefore $\eta_{b,ss}$ raises from 1 towards 2.267 (perfectly clamped case) the reduction of the main beam maximum response with respect to the unretrofitted situation drastically increases, especially for low levels of structural damping of the super-structure. In fact if ζ_B=0.5% R_{max} increases from zero reduction in the simply-supported case to approximately 87% for $\eta_{b,ss}$=1.5, that is, when the natural frequency of the auxiliary beam is increased 1.5 times its initial value thanks to restraining the end rotations. In the remaining three cases a similar tendency is observed although the results are less impressive as the retrofitting system effect on the main beam is already better in the simply-

supported case.

5 INTRODUCTION OF RAILWAY TRAFFIC EXCITATION

In the present section the effectiveness of the proposed solution and the adequacy of expressions (35) which provide the optimal dampers for a particular auxiliary beam are evaluated under railway traffic. To this end the dynamic performance of a single track bridge retrofitted with the partially clamped auxiliary beam system is investigated under the circulation of trains of moving loads which excite resonance situations in the superstructure.

In what follows the dynamic performance of a 15 m bridge is investigated using a planar FE model as the one shown in Fig. 2. The upper beam, which represents the deck, has a fundamental frequency f_{B1}=8.92 Hz and a linear mass m_B=10000 kg/m. The auxiliary beam is considered a steel element with a hollow rectangular cross-section, having L_B=L_b=L and E_b=2.1·10^{11} N/m^2. The external dimensions of the auxiliary beam are $b \times h$ (width × height) and its constant thickness is e. Thus, the second moment of area is I=(bh^3-(b-2e)(h-2e)^3)/12. The mass per unit length is m_b=ρ_b(bh-(b-2e)(h-2e)), where ρ_b=7850 kg/m^3 is the mass density of steel. Respectively, linear and quadratic variations of b and e in terms of h are adopted

$$b(h) = a \times h \qquad \text{for } a = 0.6 \tag{39}$$

$$e(h) = e_0 + e_1 \times h + e_2 \times h^2 \quad \text{for } e_0 = 2.14 \times 10^{-2}\,\text{m},\ e_1 = 7.86 \times 10^{-3},\ e_2 = 1.07 \times 10^{-2}\,\text{m}^{-1} \tag{40}$$

The dynamic response of the bridge retrofitted with a particular auxiliary beam with h=0.80 m is evaluated under the circulation of the eighth train of the High Speed Load Model –A (HSLM-A8) defined in Eurocode [35] using a moving load model. The degree of partial restriction of the auxiliary beam end section rotations is considered to be such that the fundamental frequency of the element is increased 1.5 times with respect to the simply-supported case. This corresponds to a rotational stiffness of K=4.5·10^8 Nm leading to a fundamental frequency of the auxiliary beam f_{b1}=15.87 Hz. Three dampers are introduced linking the vertical motion of corresponding sections of the main and auxiliary beams. The response of the system is computed by Modal Superposition of the first three modes of the bridge and the first three modes of the auxiliary beam. Structural damping ratios of ζ_{Bi}=1.35% and ζ_{bi}=0.5% for i=1,2,3 are assumed for each element.

In first place the adequacy of the expressions derived in the harmonic case for the external optimal damping ratios (35) is evaluated. To this end the maximum vertical acceleration at the mid-span section of the bridge is calculated under the HSLM-A8 train for circulating velocities in the range [40, 125] m/s in steps of 0.5 m/s ([144, 450] km/h in steps of 1.8 km/h). The maximum response of the bridge retrofitted with the previously described beam is computed for several values of the dampers constants and plotted in terms of accelerations in Fig. 9. The bridge in the bare case (ζ_D=0%) experiments a second and a third resonance of its fundamental mode at the theoretical velocities

$$V^{RES}_{m=1,n=2} = \frac{d_k \cdot f_{B1}}{n} \cdot 3.6 = \frac{18 \cdot 8.92}{2} \cdot 3.6 = 401.4 \text{ km/h} \tag{41}$$

$$V^{RES}_{m=1,n=3} = \frac{d_k \cdot f_{B1}}{n} \cdot 3.6 = \frac{18 \cdot 8.92}{3} \cdot 3.6 = 267.6 \text{ km/h} \tag{42}$$

being d_k=18 m the characteristic distance (or distance causing resonance) of train HSLM-A8, m the mode number, n the resonance order (or number of oscillations completed by the upper beam between the passage of repetitive groups of axle loads separated d_k). The response of the bridge has been recalculated for increasing values of the external damping ratio and,

therefore, of the individual dampers constants. If the three dampers are located at 0.25L, 0.5L and 0.75L the relation between the constants and ζ_D is given by

$$C_{Di} = \frac{1}{2} m_B L_B \omega_{B1} \zeta_D \quad \text{for} \quad i = 1,2,3 \tag{43}$$

being ω_{B1} the circular frequency of the bridge fundamental mode. As ζ_D increases the bridge response decreases, especially at resonance, and the resonant or critical velocity slightly shifts towards higher values. This kind of behaviour was already detected in the harmonic case (see Fig. 5a). When ζ_D reaches certain value the amplification at resonance starts to increase again. The theoretical optimal external damping ratio associated to the minimum acceleration at resonance has been calculated applying equation (35b) for η=1.779 and μ=0.066 (frequency and mass ratio for the particular case h=0.80 m and K=4.5·10^8 Nm) providing a value of $\zeta^*_{D,a} = 6.1\%$. In Fig. 9 the maximum acceleration of the bridge has been represented for this particular retrofitting level in red trace.

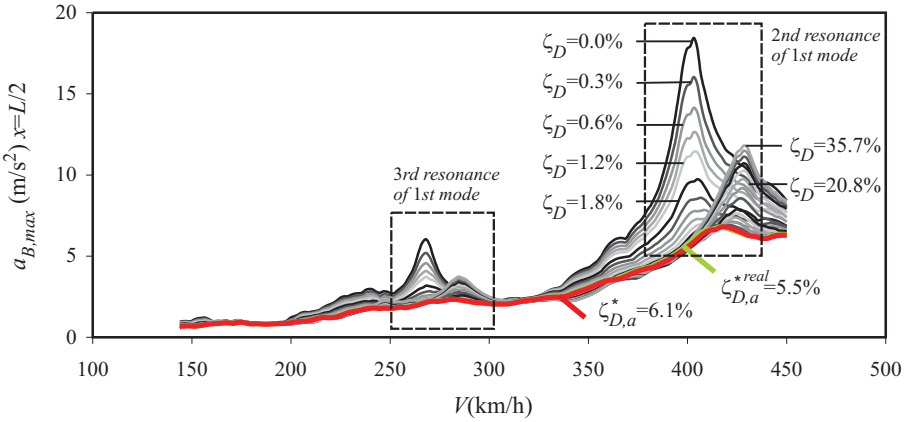

Figure 9: Maximum acceleration at bridge mid-span vs. velocity of train HSLM-A8 for different values of ζ_D.

As it can be observed equation (35b) provides a good estimate of the dampers constants real optima under the circulation of moving loads, accounting for the contribution of three modes of each beam and considering structural damping. Regarding the difference between optimal damping ratios $\zeta^*_{D,A}$ and acceleration $\zeta^*_{D,a}$ provided by equations (35a) and (35b) respectively, the former provides better estimates for the optimal dampers minimising the bridge response in terms of displacements and the latter does the same in terms of accelerations. Nevertheless the difference between both values is very small. Finally, the real value of the optimal external damping, $\zeta^{*real}_{D,a}$, has been obtained numerically as the one minimising the acceleration at the second resonance of the bridge fundamental mode being as $\zeta^{*real}_{D,a} = 5.5\%$. The bridge acceleration at mid-span for the real optimal dampers has been represented as well in green trace in Fig. 9. Even though there is a difference of 0.6% between the real and the theoretical optimal damping the difference in the bridge response is practically negligible as it can be seen when comparing the red and green curves in Fig. 9. In particular the maximum response of the bridge at the second resonance when retrofitted with the theoretical optimal dampers $a_{B,\max}\left(\zeta^*_{D,a} = 6.1\%\right) = 6.809\, m/s^2$ and when retrofitted with the real optimal dampers $a_{B,\max}\left(\zeta^{*real}_{D,a} = 5.5\%\right) = 6.801 m/s^2$.

Finally, the possibility of retrofitting the 15 m bridge so that the structure accomplishes the Serviceability Limit State of vertical acceleration (3.5 m/s^2 for ballasted tracks) is envisaged. To this end two possibilities are considered and compared: (i) connecting to the bridge deck to

a simply-supported auxiliary beam with its corresponding optimal dampers located at 0.25 L, 0.5 L and 0.75 L, and (ii) installing a partially clamped auxiliary beam with the same configuration of dampers. The aim of this analysis is to determine what would be the minimum size of the auxiliary beam needed to reduce the maximum acceleration of the bridge below 3.5 m/s^2 in each case. In the unretrofitted case the maximum acceleration of the bridge under the circulation of the HSLM-A8 train in the range of velocities [144, 450] km/h reaches 18.4 m/s^2. The steel box section beam previously described is considered for the retrofit. Beam section heights starting from 1.0 m and increasing in 10 cm increments are first considered in the simply-supported case. For each beam, nondimensional parameters μ and η are calculated and the theoretical optimal damping ratio $\zeta_{D,a}^{*}$ is obtained as per Eq. (35b). From this value the dampers constants are determined and the bridge dynamic response after the retrofit is computed. In Table 1 a summary of the retrofitting system parameters along with the maximum response of the bridge that takes place for each particular retrofit has been included.

h (m)	BC	K (Nm)	f_{b1} (Hz)	η	μ	$\zeta_{D,a}^{*}$ (%)	$a_{B,max}$ (m/s^2)
1.3	SS	---	17.20	1.928	0.155	14.21%	3.52
1.2	SS	---	15.87	1.779	0.155	10.61%	4.41
1.1	SS	---	14.54	1.630	0.155	7.45%	5.99
1.0	SS	---	13.20	1.480	0.155	4.80%	7.72
1.3	EC	2.80E+09	25.90	2.904	0.155	28.38%	2.59
1.2	EC	2.00E+09	23.80	2.668	0.155	23.23%	2.85
1.1	EC	1.47E+09	21.91	2.457	0.155	18.43%	3.17
1.0	EC	1.02E+09	19.90	2.231	0.155	13.72%	3.56

Table 1: Retrofit parameters.

In Table 1 BC, SS and EC stand for *Boundary Conditions*, *Simply-Supported* and *Elastically-Clamped*, respectively.

In Fig. (10a) the maximum acceleration of the bridge at mid-span for a simply-supported auxiliary beam of section heights varying from 1.0 m to 1.3 m has been represented.

It is important to stress that each auxiliary beam is combined with the dampers that lead to the super-structure minimum response, that is, with the optimal dampers. As it is shown a minimum height of 1.3 m is needed for the maximum acceleration to reduce until the limit 3.5 m/s^2 if the beam is simply-supported. The same calculations are repeated considering that the beam is partially clamped. The rotational stiffness is supposed to be the same at both ends and such that the fundamental frequency of the auxiliary beam increases 1.5 times its corresponding value in the simply-supported case. In Fig. (10b) the maximum acceleration of the bridge is plotted for each particular beam size in the elastically-clamped case. The response of the bridge drastically reduces for a particular retrofit if the auxiliary beam ends rotations are restrained. It can be observed that if the beam is partially clamped a beam with a section height of 1 m would be sufficient for the bridge to accomplish the Serviceability State of vertical acceleration, while in the simply-supported case a 1.3 m beam was needed.

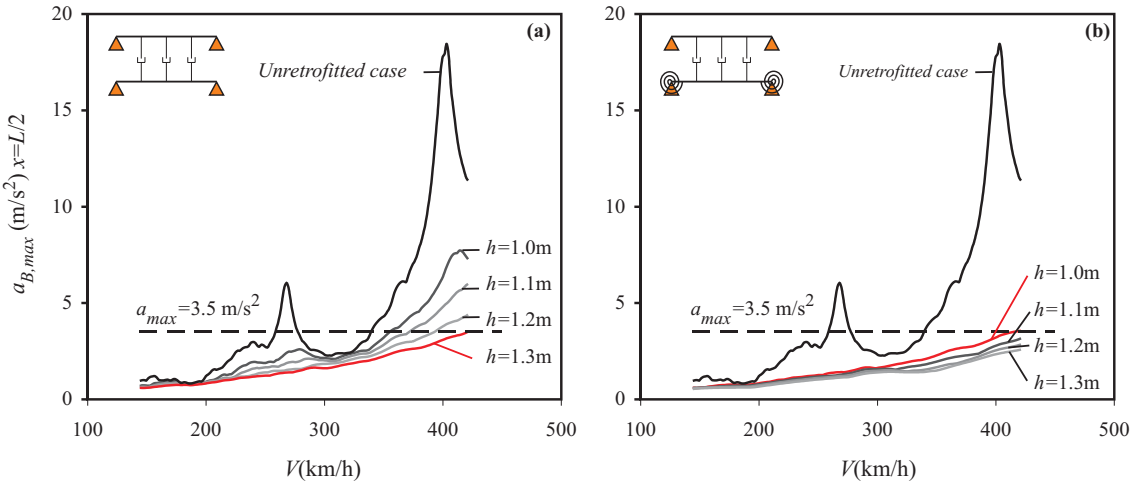

Figure 10: Maximum acceleration at bridge mid-span vs. velocity of train HSLM-A8 for different auxiliary beam sizes in the (a) simply-supported and (b) elastically clamped cases.

6 CONCLUSIONS

The dynamic performance of simply supported beams retrofitted with FVDs and subjected to moving loads has been evaluated. The main beam, which supports the passage of the loads, is connected to an auxiliary beam placed parallel to the former through a set of dampers linking the vertical motion of corresponding sections of the elements. The auxiliary beam is considered to be partially clamped at both ends. From the results obtained herein, the following conclusions can be derived:

- (i) The resonant vibrations that may appear in simply supported beams when subjected to moving loads can be drastically reduced with the damping system proposed herein.
- (ii) For a particular auxiliary beam, there exists an optimum value of the FVD constants that minimise the main beam response.
- (iii) The main beam response monotonically reduces with the auxiliary beam mass and natural frequency, but, in order for the dampers to effectively dissipate energy, the auxiliary beam fundamental frequency must exceed the main beam modal frequency which contribution is to be reduced.
- (iv) The design strategy should be to select the smallest auxiliary beam such that when associated with its corresponding optimal FVDs leads to the desired system performance.
- (v) Partially restraining the rotation of the auxiliary beam supports leads to an important reduction of the main beam response at resonance when compared to the simply-supported case. This permits to reduce the size of these elements which are to be installed underneath the deck in general applications.
- (vi) Analytical expressions for the optimal damper constants are provided which provide very accurate results as long as the maximum response of the main beam in the range of evaluated velocities occurs at resonance.

- (vii) With the system proposed in this article the FVDs need not interact with the upper side of the bridge. This allows existing railway bridges to be retrofitted while keeping the line in operation.
- (viii) The damping system and optimal damper expressions presented here may apply to other situations where simply supported beams vibrate at resonance due to different causes.

REFERENCES

[1] European Rail Research Institute, *PontsRails pour vitesses > 200 km/h. Rapport final*. ERRI D-214/RP9, 2000.

[2] Ministerio de Fomento, *Instrucción sobre las acciones a considerar en el proyecto de puentes de ferrocarril* (IAPF-07). Ministerio de Fomento, 2007.

[3] Fryba L. *Dynamics of bridges under moving loads. Past, present and future*. Workshop: Dynamics of High-Speed railway bridges, R. Delgado, R. Calçada, J.M. Goicolea and F. Gabaldón eds., Porto, 2005; 25–44.

[4] Mancel F. *Cedypia: Analytical software for calculating dynamic effects on railway bridges*. In: Proc. Fourth European conference on Structural Dynamics (Eurodyn'99), Vol. 2, Prague, 1999; 675–680.

[5] Kwon HC, Kim MC, Lee IW. *Vibration control of bridges under moving loads*. Comput Struct 1998; 66:473–480.

[6] Wang JF, Lin CC, Chen BL, *Vibration suppression for High-Speed railway bridges using tuned mass dampers*. Int J Solids Struct 2003; 40:465–491.

[7] Yau JD, Yang YB. *Vibration reduction for cable-stayed bridges travelled by High-Speed trains*. Finite Elem Anal Des 2004; 40:341–359.

[8] Yau JD, Yang YB. *A wideband MTMD system for reducing the dynamic response of continuous truss bridges to moving train loads*. Eng Struct 2004; 26:1795–1807.

[9] Yau JD. *Train-induced vibration control of simple beams using string-type tuned mass dampers*. J Mech 2007; 4:329–340.

[10] Li J, Su M, Fan L. *Vibration control of railway bridges under High-Speed trains using multiple tuned mass dampers*. J Bridge Eng 2005; 10:312–320.

[11] Samani F.S., Pellicano F., *Vibration reduction on beams subjected to moving loads using linear and nonlinear dynamic absorbers*. J Sound Vib 2009; 325:742–754.

[12] Minsili LS, Zhong T, Xia H, Manguelle DE. *Design and vibration control by friction dampers in truss bridges*. In: Proc. of the Second International Conference on Construction in Developing Countries: Challenges Facing the Construction Industry in Developing Countries 2002.

[13] Choo JF, Koh HM, Kang SC, Kim BS. *Vibration control of long-span High-Speed railway bridges under periodic moving loading using viscoelastic damper*. In: Structures for High-speed Railway Transportation, International Association for Bridge and Structural Engineering 2003.

[14] Vu HV, Ordóñez AM, Karnopp BH. *Vibration of a double-beam system*. J Sound Vib 2000; 229:807–822.

[15] Abu-Hilal M. *Dynamic response of a double Euler-Bernoulli beam due to a moving constant load. J Sound Vib 2006; 297:477–491.*

[16] *Oniszczuk Z. Free transverse vibrations of elastically connected simply supported double-beam complex system*. J Sound Vib 2000; 232:387–403.

[17] Oniszczuk Z. *Forced transverse vibrations of an elastically connected complex simply supported double-beam system*. J Sound Vib 2003; 264:273–286.

[18] Oniszczuk Z. *Free transverse vibrations of an elastically connected rectangular simply supported double-beam plate system*. J Sound Vib 2000; 236:595–608.

[19] Oniszczuk Z. *Forced transverse vibrations of an elastically connected complex rectangular simply supported double-beam plate system*. J Sound Vib 2004, 270:997–1011.

[20] Moliner E, Martínez-Rodrigo MD, Lavado J. *Vibration control of high-speed railway bridges using viscoelastic dampers*. In: Proc. of the Eleventh International Conference on civil, Structural and Environmental Engineering Computing 2007.

[21] Moliner E, Museros P, Martínez-Rodrigo MD. *Vibration control of high-speed railway bridges using viscoelastic dampers modelled by means of fractional derivatives*. In: Proc. of the International conference on noise and vibration engineering 2008, 2867-2877.

[22] Oliveto G, Santini A, Tripodi E. *Complex modal analysis of a flexural vibrating beam with viscous end conditions*. J Sound Vib 1997; 200:327–345.

[23] Greco A, Santini A. *Dynamic response of a flexural non-classically damped continuous beam under moving loadings*. Comput Struct 2002; 80:1945–1953.

[24] Taylor DP, Lee DA. *Frictionless damper*. United States Patent number 4.815.574, 1989.

[25] Martínez-Rodrigo MD. *Atenuación de vibraciones resonantes en puentes de ferrocarril de Alta Velocidad mediante amortiguadores fluido-viscosos*. PhD Thesis. Universidad Politénica de Valencia, 2009.

[26] Museros P, Martinez-Rodrigo MD. *Vibration control of simply supported beams under moving loads using fluid viscous dampers*. J Sound Vib 2007; 300:292–315.

[27] Martinez-Rodrigo MD, Museros P. *Optimal design of passive viscous dampers for controlling the resonant response of orthotropic plates under high-speed moving loads*. J Sound Vib 2010; doi:10.1016/j.jsv.2010.10.017.

[28] Martínez-Rodrigo MD, Lavado J, Museros P. *Dynamic performance of existing high-speed railway bridges under resonant conditions retrofitted with fluid viscous dampers*. Eng Struct 2010; 32:808–828.

[29] European Committee for Standardisation (CEN). *Eurocode: Basis of structural design. Annex A2: Application for bridges*. Final Draft prEN 1990 prAnnex A2 (pre-European Standard) 2002.

[30] Frýba L. *A rough assessment of railway bridges for high speed trains*. Eng Struct 2001; 23:548–556.

[31] Frýba L. *Dynamics of solids and structures under moving loads*. Thomas Telford, 1999.

[32] Olsson M. *On the fundamental moving load problem*. J Sound Vib 1991; 145: 299–307.

[33] Yang YB, Yau JD, Hsu LC. *Vibration of simple beams due to trains moving at high speeds*. Eng Struct 1997; 19: 936–944.

[34] Museros P, Alarcón E. *Influence of the second bending mode on the response of high-speed bridges at resonance*. J Struct Eng-ASCE 2005; 131:405–415.

[35] European Committee for Standardisation (CEN). *Eurocode 1: Actions on structures. Part 2: traffic loads on bridges*. Final Draft prEN 1991-2 (pre-European Standard) 2002.